# Supporting Information

## A covalently attached progesterone molecule outcompetes the binding of free progesterone at an allosteric site of cytochrome P450 3A4

Julie Ducharme, Vanja Polic, Karine Auclair*

Department of Chemistry, McGill University, Montreal, Canada

## Supporting methods

### 1) General

All chemicals and reagents were purchased from Sigma-Aldrich Canada Ltd. (Oakville, ON, Canada), Alfa Aesar (Ward Hill, MA, USA), Chem-Impex (Wood Dale, IL, USA), Agilent Technologies Canada Inc. (Mississauga, ON, Canada) or BioRad (Mississauga, ON, Canada) and were used without further purification. The mutagenesis kit and sequencing primers were obtained from Life Technologies. The CYP3A4 and CPR expression plasmids were generously provided by Dr. J. R. Halpert (University of Connecticut) and Dr. C. B. Kasper (University of Wisconsin-Madison), respectively.

### 2) Site-directed mutagenesis, mutants' generation

Mutants with a single reactive cysteine were generated using the PCR kit QuickChange II XL (Agilent) from the plasmid of a reported cysteine-depleted CYP3A4 mutant (C58T/C64A/C98S/C239S/C468G).[1] The WT CYP3A4 is a *N*-terminally truncated mutant expressed from the pSE3A4His plasmid.[2] Sequence of the primers (Life Technologies) used in site-directed mutagenesis are listed in **Figure S12**. All mutations were confirmed through Sanger DNA sequencing by Genome Quebec (Montreal, Canada).

### 3) CYP3A4 WT and mutant's expression and purification

CYPs expression and purification was performed as previously described, with the following modifications.[1] Protein expression was induced at $OD_{600}$ = 0.6 – 0.8. The TB growth medium was supplemented with trace metals[3] and cell were harvested at 5000 × *g* for 10 min. Pellets of 100-150 g were resuspended in potassium phosphate buffer (0.05 M pH 7.4, 10% glycerol) to reach a final volume of about 250 ml. This 0.05 M KPi buffer was also used to equilibrate the Ni-NTA resin agarose resin (15 ml, Qiagen) and throughout the whole purification. After incubation with lysis buffer, the dissolved pellet was aliquoted into six 50 ml beakers and the sonication was performed at 80% cycle duty instead of 60%. After elution from the Macro-Prep High S resin (BioRad), the protein was dialyzed against a higher concentration of phosphate buffer (0.1 M, pH 7.4, 10% glycerol). The protein was concentrated using Corning Spin-X UF concentrators (30K, Millipore Sigma) to decrease the final volume to about 10 ml or until the color of the

protein solution becomes dark orange-red. Typically, the CYP concentration obtained varies between 10-20 μM and the protein yield between 0.1 – 1 mg $L^{-1}$ culture.

**4) Cytochrome P450 Reductase (CPR) expression and purification**

The expression and purification of CPR was achieved as previously described except for one modification in the expression protocol.[1] At the inoculation stage, each 2L flask of LB growth medium was supplemented with 5 ml of riboflavin solution (0.2mg/ml, 50:50 ACN:H2O, pH 11).

**5) CYP3A4 mutants bioconjugation**

Purified mutants were covalently labeled with different maleimide reagent as published earlier.[1,4] Briefly, the CYP3A4 single cysteine mutants (2 μM) were individually incubated with TCEP (45 μM from a 10 mM stock in MilliQ) for 20 minutes at r.t. on an orbital shaker (50 rpm). Bioconjugation was initiated with the addition of the maleimide reagent (100 μM from a 20 mM stock in anhydrous DMSO) and the reaction was allowed to proceed for 2 hours at 4°C with gentle shaking (50 rpm). The reaction was quenched with DTT (2 mM from a 100 mM stock in MilliQ) for 10 min at r.t. The total reaction volumes ranged from 200-700 μl. Controls were always run in parallel and consisted of the same reaction mixture, treated the same way but with the addition of pure DMSO instead of the maleimide reagent in DMSO. Excess reagent and quenched maleimide were removed by eluting the final mixture through a Zeba Spin Desalting Column (1 x 2ml, Pierce) pre-equilibrated with KPi buffer (0.1 M, pH 7.4 10% glycerol). The desalted samples were always used fresh. All the maleimide reagents were commercially available (ThermoFisher Scientific), except for the PGM which was synthesized as previously described[1].

**6) Bioconjugation yield**

The protein sample (50-300 μl, 2 μM) was washed with MilliQ $H_2O$ (3 X 0.5 ml) using Spin-X concentrator (30 K MWCO, 0.5ml, Corning) for 3 × 15 min at 15,000 × *g*. The full-length protein was analyzed by LC-MS-QToF as previously described.[1]

**7) BFC debenzylation *assay***

***Activity assay*** The activity of CYP3A4 mutants and bioconjugates was determined by measuring initial rates for enzyme-catalyzed debenzylation of BFC to HFC using a microtiter plate with fluorescence detection. The assay was performed in a potassium phosphate buffer (0.1 M, pH 7.4, 10% glycerol) containing CYP3A4 (0.4-0.8 μM), CPR (0.8-1.6 μM), BFC (16.5-33 μM from an initial stock of 3.3 mM in ACN) and NADPH (1 mM from a stock of 25 mM in MilliQ water) for a total reaction volume of 150 μl. The final DMSO concentration was always below 1%. Prior to initiating the reaction with addition of NADPH, the reaction mixture was pre-mixed and incubated for 5 minutes at 37°C. Following NADPH addition, HFC production was monitored over 1h (Ex/Em: 410 nm/530 nm). The initial rates were obtained from calculating the slope of the linear portion of the kinetic curve and the RFU were converted into nM/s using an HFC calibration curve.

***Michaelis Menten Kinetics*** Enzyme kinetics with BFC were determined by varying the BFC concentration and keeping the other reaction components constant. The reaction mixtures

contained CYP3A4 (0.7 μM), BFC (10-100 μM from initial stocks of 1-10 mM in DMSO) in KPi buffer (0.1 M, pH 7.4, 10% glycerol), CPR (0.7 μM) and NADPH (1 mM from a stock of 25 mM in MilliQ). The final concentration of DMSO added was 1% of the total volume at most. To decrease sample variabilities due to pipetting errors, master mixes of the enzyme were prepared (KPi buffer, CYP3A4, CPR). Then each master mix was aliquoted in six portions accounting for the six different BFC concentration tested. BFC was added to each portion before incubation for 5 min at 37°C and 250 rpm. The mixes were next aliquoted (3 × 144 μl) and each individual reaction was initiated with the addition of NADPH. The final reaction volume was 150 μl. The formation of HFC was monitored over 30 min (Ex/Em: 410 nm/530 nm) to obtain the initial linear portion of each kinetic curve. These rates obtained in RFU were converted into nM/s using the HFC calibration curve. For each BFC concentration, a slope was calculated from the initial reaction rate. A better fit was obtained using the Hill equation than with the Michaelis-Menten equation, and hence the former was applied to derive the kinetics parameters ($K_M$, $V_{max}$ and the Hill coefficient) using GraphPad Prism. The turnover number, $k_{cat}$, was calculated by dividing the $V_{max}$ with the enzyme concentration, and the specificity constant is defined as $k_{cat}/K_M$ . (**Figures S12 and S14**).

**8) Progesterone activation assay**

The extent of progesterone (PRG) activation of enzyme-catalyzed BFC debenzylation was evaluated by comparing the initial rates of HFC production in the presence of PRG at different concentrations. The desired unmodified mutants or bioconjugate (0.7 μM) was dissolved in KPi buffer (0.1 M, pH 7.4, 10% glycerol) along with CPR (0.7 μM), BFC (50 μM from a 30 mM stock solution prepared in DMSO) and PRG (0-25 μM from 0.25-2.5 mM stock solutions in DMSO). In the samples with no PRG, DMSO was added instead. The total concentration of DMSO in samples was 1% at most. To decrease sample variabilities due to pipetting errors, master mixes of the enzyme were prepared (KPi buffer, CYP3A4, CPR, BFC). Then each master mix was aliquoted in six portions accounting for the six different PRG concentrations tested. PRG was added to each before incubation for 5 min at 37°C and 250 rpm. The mixes were aliquoted (3 x 144 μl) and each individual reaction was initiated with the addition of NADPH (1 mM). The final reaction volume was 150 μl. The HFC production rates were monitored over 30 min (Ex/Em: 410 nm/530 nm) in order to obtain the linear first portion of the kinetic curve. These rates, obtained in RFU, were converted into nM/s using an HFC calibration curve. For each PRG concentration, a slope was calculated from the initial reaction rate and plotted against PRG concentration using exponential functions in GraphPad Prism. The HFC production rates of the enzyme without PRG activator were compared to the maximum activation at 25 μM to obtain an activation ratio (**Figure S14**).

## Supporting figures

| Residues | Distance with PRG (Å) |
|---|---|
| F108 (Mut1) | 10.0 |
| G481 (Mut2) | 11.8 |
| L482 (Mut3) | 11.5 |
| V111 (Mut4) | 11.0 |
| Q484 (Mut5) | 15.0 |
| F215 (Mut6) | 9.2 |
| I301 (Mut7) | 13.6 |
| F304 (Mut8) | 10.9 |
| L210 (Mut9) | 10.1 |
| Heme | 18.3 |

| Other elements | Length (Å) |
|---|---|
| PRG | 11.7 |
| PGM | 15.5 |

**Figure S1.** *Left*: distance between the co-crystallized progesterone molecule crystallized in the putative allosteric site of P450 3A4 (PDB: 1W0F)[5] and the mutated residues. The distances are measured from the first carbon in the amino acid side chain to the carbon at position 16 on the steroid backbone of progesterone. The first six residues are the successful bioconjugated mutants. *Right*: the length of the progesterone (PRG) and the progesterone-maleimide (PGM) molecules are also given as reference points.

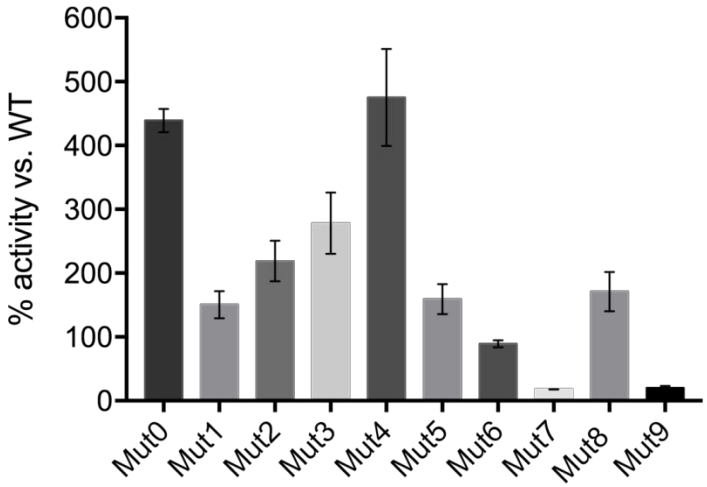


**Figure S2.** BFC activity of P450 3A4 mutant compared to WT. The activity reported is initial rate relative to that of WT, for reaction mixtures consisting of 0.4 μM P450, 1.6 μM CPR, 33 μM BFC and 1 mM NADPH. Error bars represent standard deviation of duplicates or triplicates. Interestingly, most mutants are more active than WT, but less active than mut0.

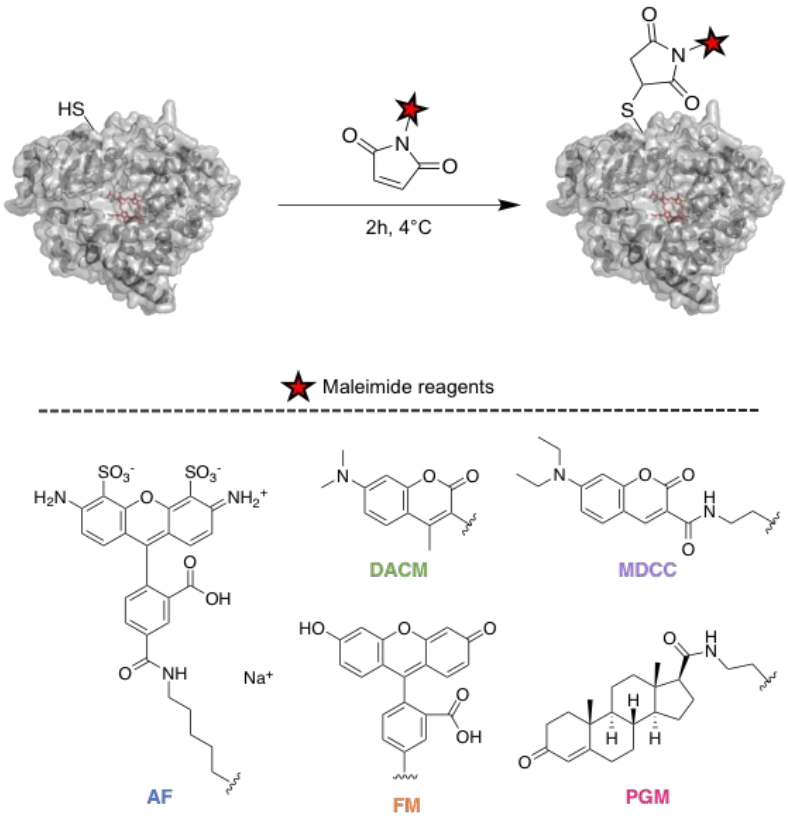


| Mutant | Theoretical mass (Da) |
|---|---|
| Mut1 | 56625.11 |
| Mut2 | 56715.24 |
| Mut3 | 56659.13 |
| Mut4 | 56673.16 |
| Mut5 | 56644.16 |
| Mut6 | 56625.11 |
| Mut7 | 56659.13 |
| Mut8 | 56625.11 |
| Mut9 | 56659.13 |

| Maleimide reagent | Molecular weight ($gmol^{-1}$) |
|---|---|
| FM | 427.36 |
| AF | 720.66 |
| PGM | 438.25 |
| DACM | 298.10 |
| MDCC | 383.15 |

**Figure S3.** Maleimide reagents used for bioconjugation. *Top*: Bioconjugation reaction scheme. The thiol group from the newly installed cysteine reacts with a maleimide handle linked to a fluorophore or a ligand analogue. Below are the structures for the maleimide reagents that were tested: Alexa fluor 488 $C_5$ maleimide (AF), *N*-(7-dimethylamino-4-methylcoumarin-3-yl)maleimide (DACM), fluorescein-5-maleimide (FM) and 7-diethylamino-3-((((2-maleimidyl)ethyl)amino)carbonyl)coumarin (MDCC). *Bottom*: tables listing the expected masses of unmodified P450 mutants, as well as the masses of the maleimide reagents. The theoretical protein average mass was

determined using the Compute pI/Mw Tool from ExPaSy: Bioinformatics Resource Portal.

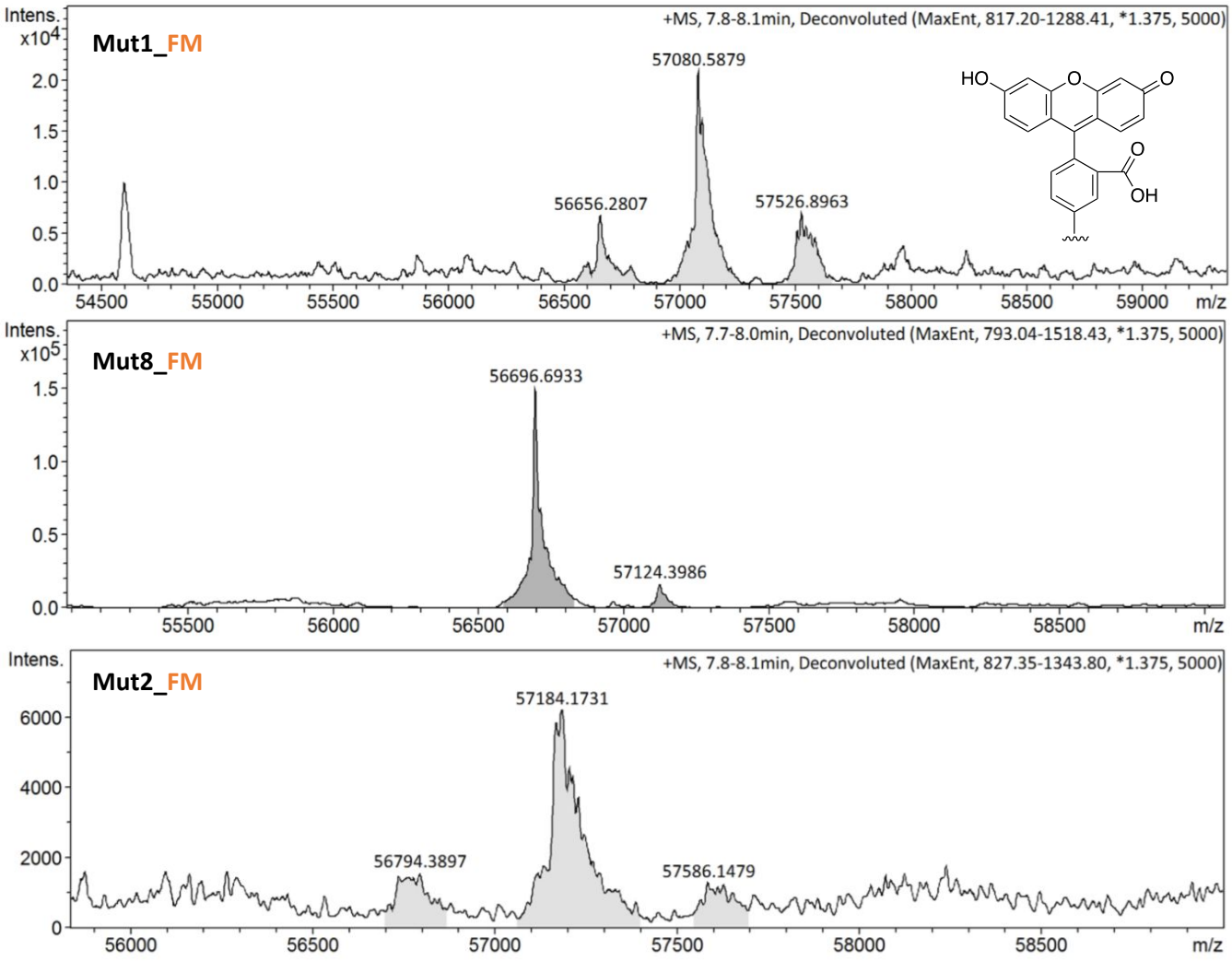


**Figure S4a.** Deconvoluted mass spectra of P450 3A4 mutants bioconjugated to FM. Refer to Figure S3 for theoretical masses of the unlabeled mutants and the mass of the FM label. Peaks correspond either to the unlabeled or the FM, singly- or doubly-labeled protein.

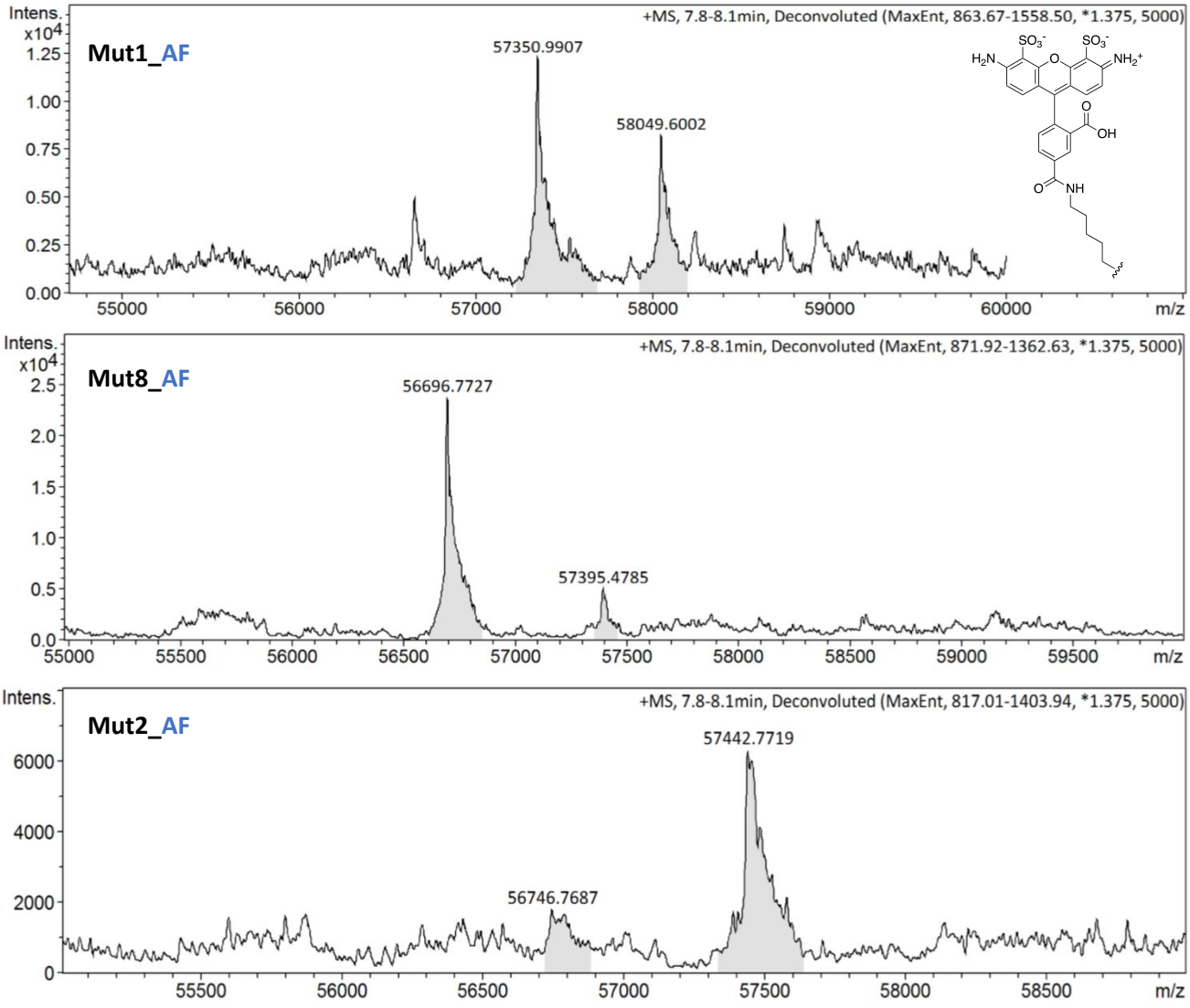


**Figure S4b.** Deconvoluted mass spectra of P450 3A4 mutants bioconjugated to AF. Refer to Figure S3 for theoretical masses of the unlabeled mutants and the mass of the AF label. Peaks correspond either to the unlabeled or the AF, singly or multiply-labeled protein.

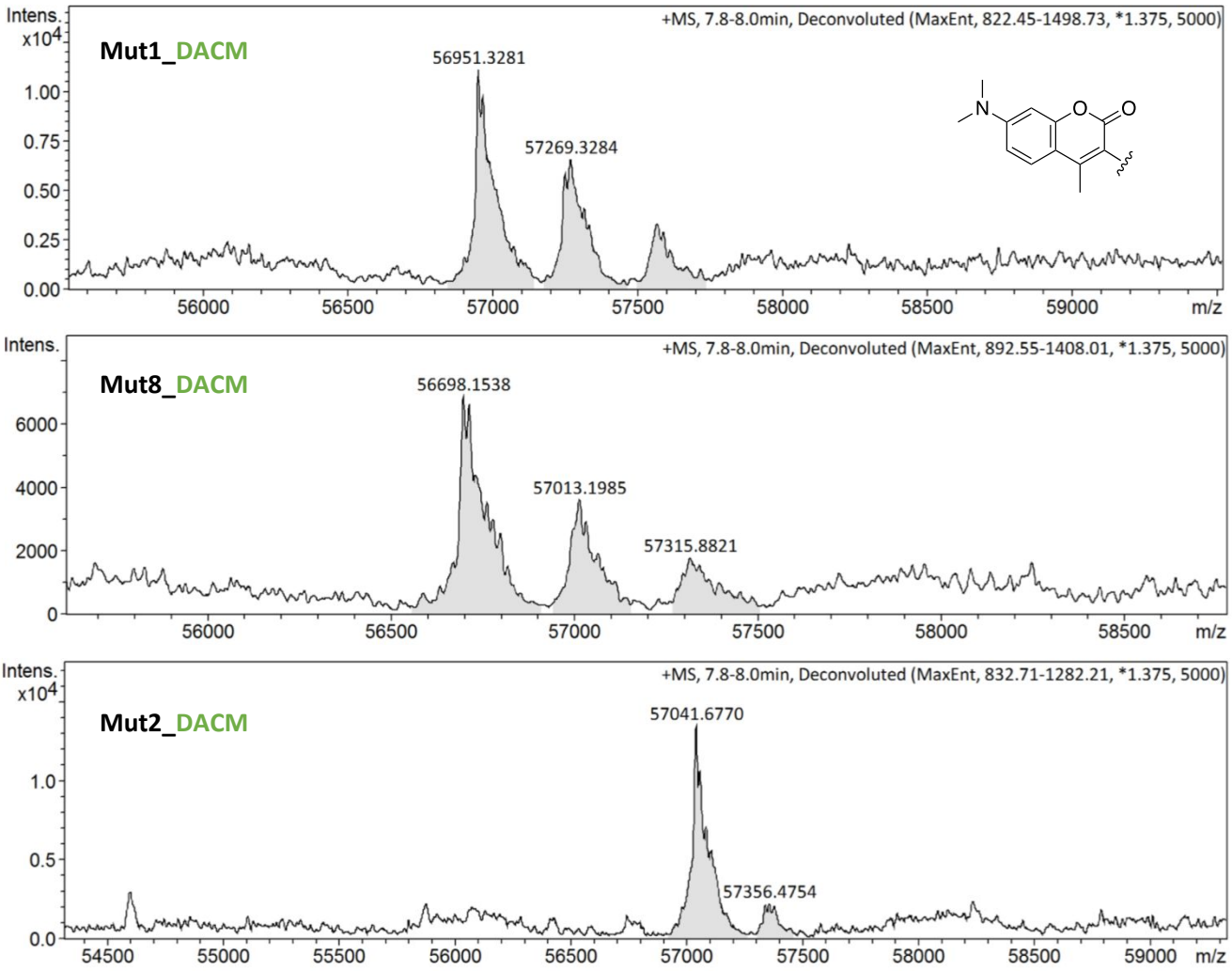


| Mutant | | FM | | | AF | | | DACM | | |
|---|---|---|---|---|---|---|---|---|---|---|
| | | 0 label | 1 label | 2 labels | 0 label | 1 label | 2 labels | 0 label | 1 label | 2 labels |
| Mut1 | % yield | 21 | 53 | 26 | 8 | 55 | 37 | 55 | 31 | 14 |
| | STD | 2 | 10 | 8 | 11 | 7 | 5 | 3 | 1 | 2 |
| Mut8 | % yield | 91 | 9 | 0 | 82 | 18 | 0 | 49 | 32 | 19 |
| | STD | 1 | 1 | 0 | 0 | 0 | 0 | 6 | 4 | 3 |
| Mut2 | % yield | 24 | 69 | 7 | 22 | 78 | 0 | 0 | 84 | 16 |
| | STD | 10 | 0 | 10 | - | - | - | 0 | 3 | 3 |

**Figure S4c.** *Top*: Deconvoluted mass spectra of P450 3A4 mutants bioconjugated to DACM. Refer to Figure S3 for theoretical masses of the unlabeled mutants and the mass of the DACM label. Peaks correspond either to the unlabeled or the DACM, singly or multiply-labeled protein. *Bottom*: FM, AF and DACM bioconjugation yields. The % yield was calculated from peak intensity, assuming that the different labeling events did not significantly affect the ionization capabilities of the protein molecule. The standard deviations (STD) are from duplicates unless indicated by a dash.

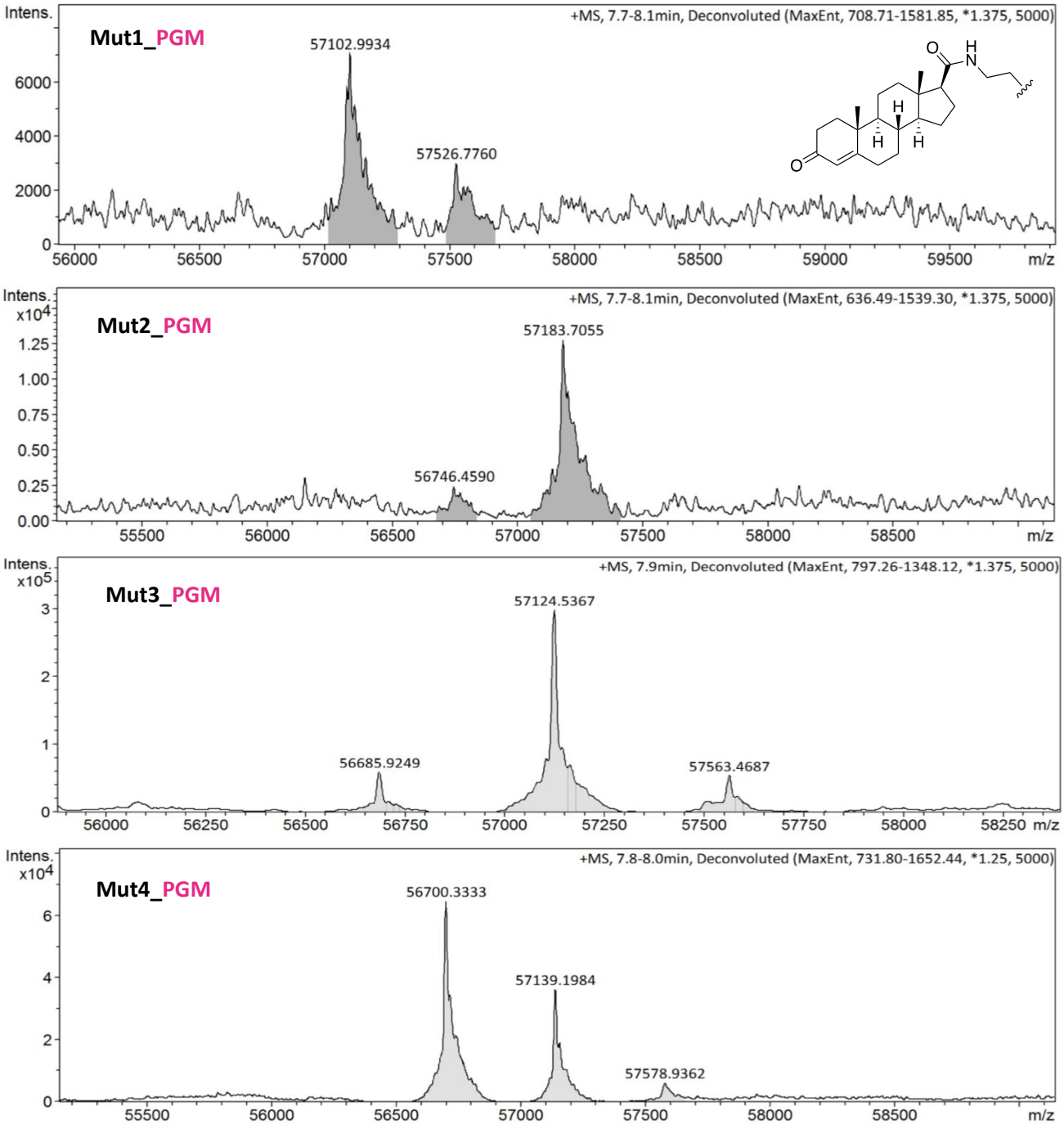


**Figure S5a.** Deconvoluted mass spectra of P450 3A4 mutants bioconjugated to PGM. Refer to Figure S3 for theoretical masses of the unlabeled mutants and the mass of the PGM label. Peaks correspond either to the unlabeled or the PGM, singly or multiply-labeled protein.

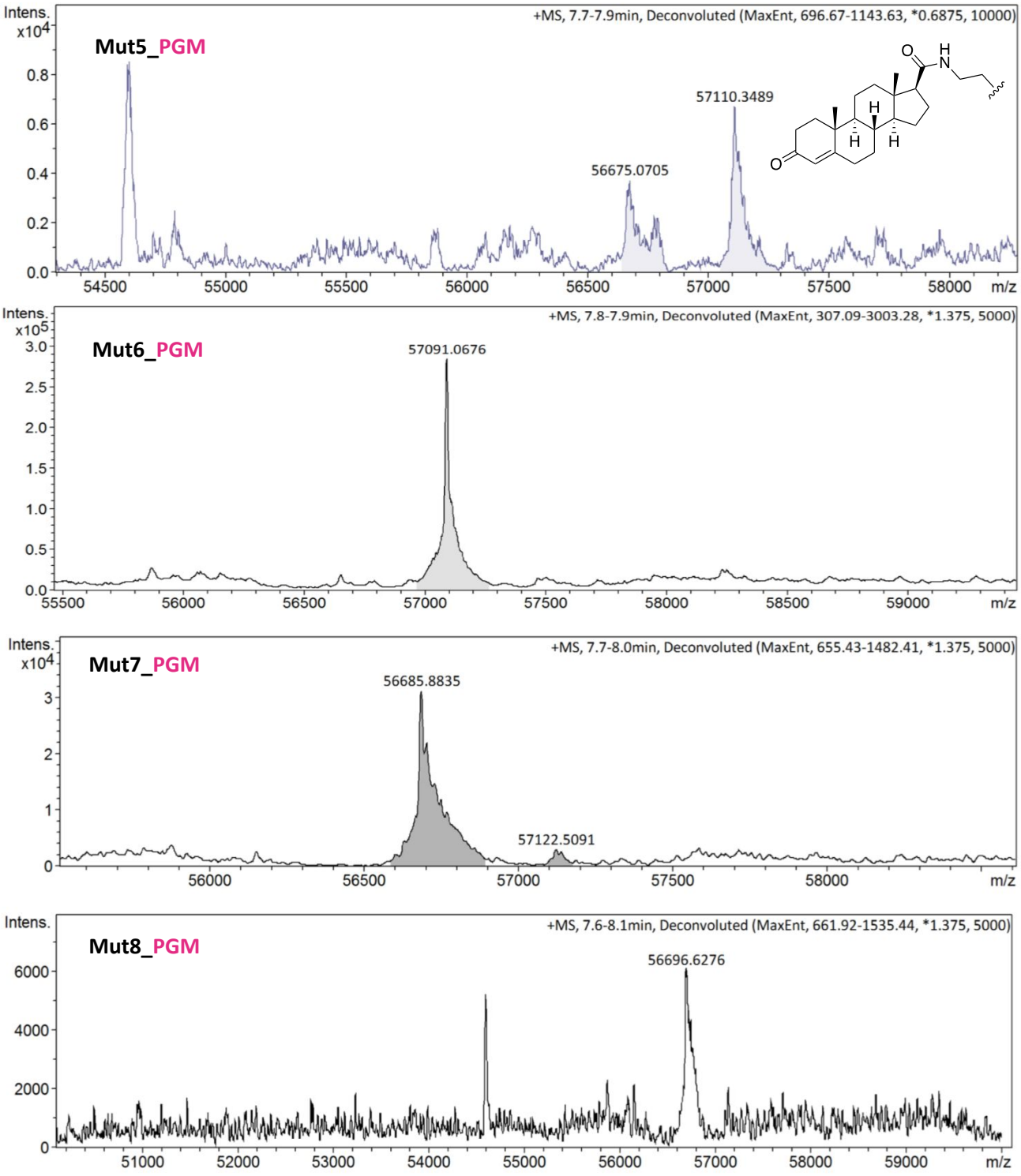


**Figure S5b.** Deconvoluted mass spectra of P450 3A4 mutants bioconjugated to PGM. Refer to Figure S3 for theoretical masses of the unlabeled mutants and the mass of the PGM label. Peaks correspond either to the unlabeled or the PGM, singly or multiply-labeled protein.

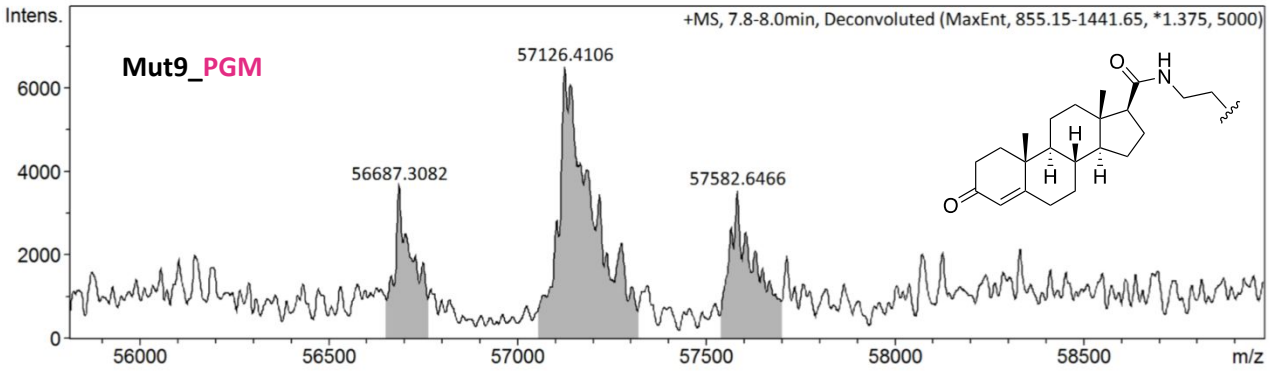


| Mutant | | PGM | | |
|---|---|---|---|---|
| | | 0 label | 1 label | 2 labels |
| Mut1 | % yield | 0 | 71 | 29 |
| | STD | 0 | 0.5 | 0.5 |
| Mut2 | % yield | 17 | 83 | 0 |
| | STD | 1 | 1 | 0 |
| Mut3 | % yield | 21 | 57 | 21 |
| | STD | 10 | 21 | 12 |
| Mut4 | % yield | 52 | 42 | 6 |
| | STD | 12 | 12 | 0 |
| Mut5 | % yield | 45 | 55 | 0 |
| | STD | 13 | 13 | 0 |
| Mut6 | % yield | 0 | 100 | 0 |
| | STD | - | - | - |
| Mut7 | % yield | 91 | 9 | 0 |
| | STD | 0 | 0 | 0 |
| Mut8 | % yield | 100 | 0 | 0 |
| | STD | 0 | 0 | 0 |
| Mut9 | % yield | 27 | 47 | 26 |
| | STD | - | - | - |

**Figure S5c.** *Top*: Deconvoluted mass spectra of P450 3A4 mutants bioconjugated to PGM. Refer to Figure S3 for theoretical masses of the unlabeled mutants and the mass of the PGM label. Peaks correspond either to the unlabeled or the PGM, singly or multiply-labeled protein. *Bottom*: PGM bioconjugation yields. The % yield was calculated from peak intensity, assuming that the different bioconjugation events did not significantly affect the ionization capabilities of the protein molecule. The standard deviations (STD) are from duplicates unless indicated by a dash. There was not attempt at purifying the labeled mutant from the unlabeled.

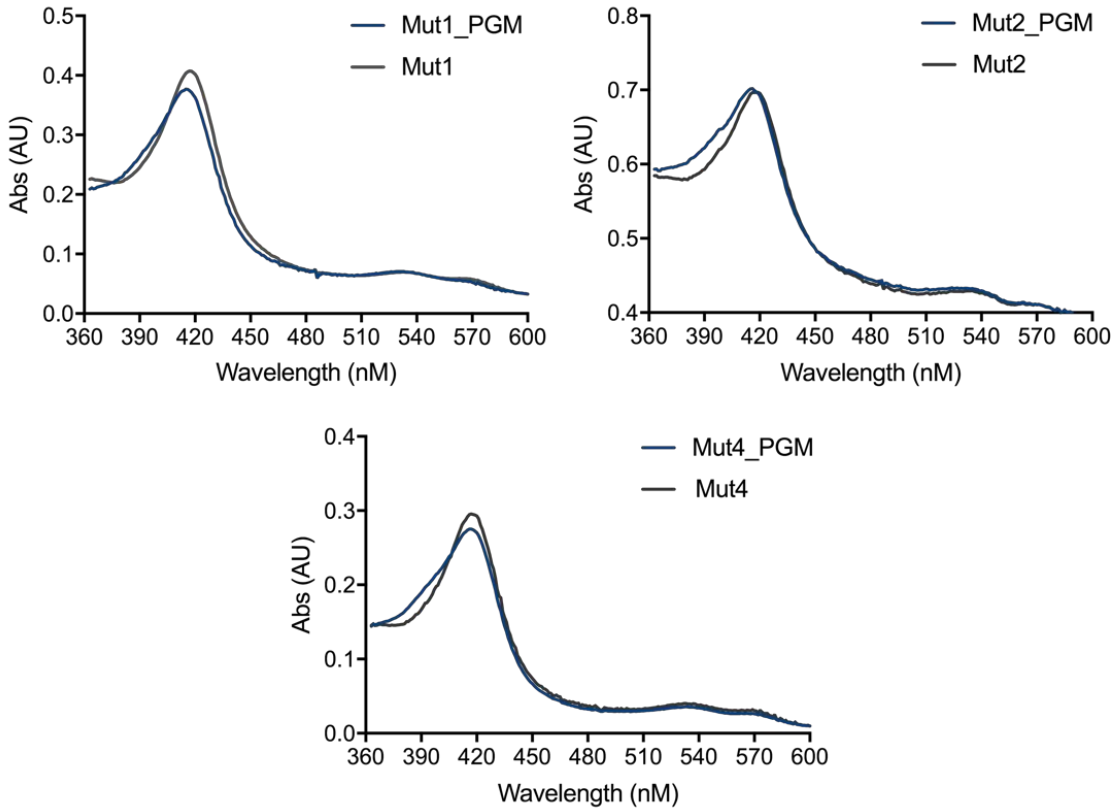


**Figure S6.** Absorbance spectra of mut1, mut2 and mut4 PGM-bioconjugates. The UV trace in gray represent the unlabeled mutant and the trace in blue represent the PGM-labeled mutant. Mut6 PGM-bioconjugate absorbance spectra was previously published.[6] In all these cases, an increase in absorbance at 390 nm was observed indicating that PGM slightly enhance the high spin state CYP3A4 population.

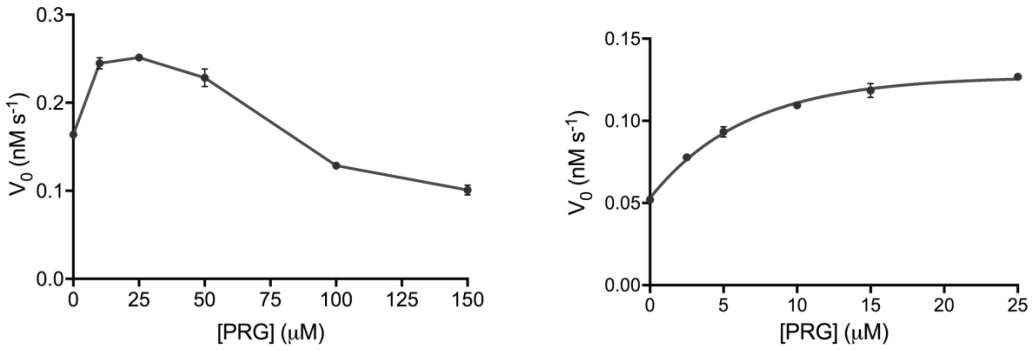


**Figure S7.** PRG activation of P450 3A4 WT. *Left:* optimization of PRG activation range with 0.7 μM P450, 0.7 μM CPR, 50 μM BFC and 1 mM NADPH. From this curve, activation is observed at 0–25 μM PRG. At higher concentrations, PRG starts to compete with BFC for oxidation and HFC production decreases. *Right:* WT activation in the optimized PRG concentration range. The reaction rate is approximately doubled at 25 μM PRG. $V_0$ represent the rate of HFC production and error bars are standard deviations for triplicates.

| Mutants | Initial rate | Activated rate | Fold activation | PGM prevent activation |
|---|---|---|---|---|
| Mut1 | 0.126 ± 0.002 | 0.222 ± 0.008 | 1.76 ± 0.07 | Y |
| Mut1_PGM | 0.334 ± 0.004 | 0.337 ± 0.001 | 1.01 ± 0.01 | |
| Mut2 | 0.141 ± 0.000 | 0.291 ± 0.005 | 2.06 ± 0.04 | Y |
| Mut2_PGM | 0.143 ± 0.001 | 0.146 ± 0.002 | 1.02 ± 0.02 | |
| Mut3 | 0.030 ± 0.001 | 0.096 ± 0.015 | 3.16 ± 0.50 | N |
| Mut3_PGM | 0.076 ± 0.002 | 0.121 ± 0.008 | 1.59 ± 0.11 | |
| Mut4 | 0.305 ± 0.010 | 0.511 ± 0.009 | 1.67 ± 0.06 | N |
| Mut4_PGM | 0.616 ± 0.005 | 0.756 ± 0.012 | 1.23 ± 0.02 | |
| Mut5 | 0.075 ± 0.001 | 0.113 ± 0.002 | 1.50 ± 0.04 | N |
| Mut5_PGM | 0.056 ± 0.002 | 0.086 ± 0.003 | 1.54 ± 0.08 | |
| Mut6 | 0.106 ± 0.001 | 0.202 ± 0.019 | 1.90 ± 0.18 | Y |
| Mut6_PGM | 0.426 ± 0.011 | 0.411 ± 0.007 | 0.97 ± 0.03 | |
| WT | 0.052 ± 0.002 | 0.127 ± 0.002 | 2.44 ± 0.09 | - |

**Figure S8.** PRG activation results. Initial rates (in nM $s^{-1}$) are calculated by averaging the triplicates of the rates obtained when 0 μM PRG is used. Activated rates (in nM $s^{-1}$) are calculated by averaging the rates at 25 μM PRG (derived from an exponential curve fit). The fold activation was calculated from the ratio of activated and initial rates. Finally, allosteric site is occupied (Y) by the PGM moiety of the bioconjugate if the free PRG has no activation effect. If the activation is observed even with bioconjugation, the PGM moiety is not likely occupying the same site as free PRG (N). The error bars represent standard deviations from triplicates.

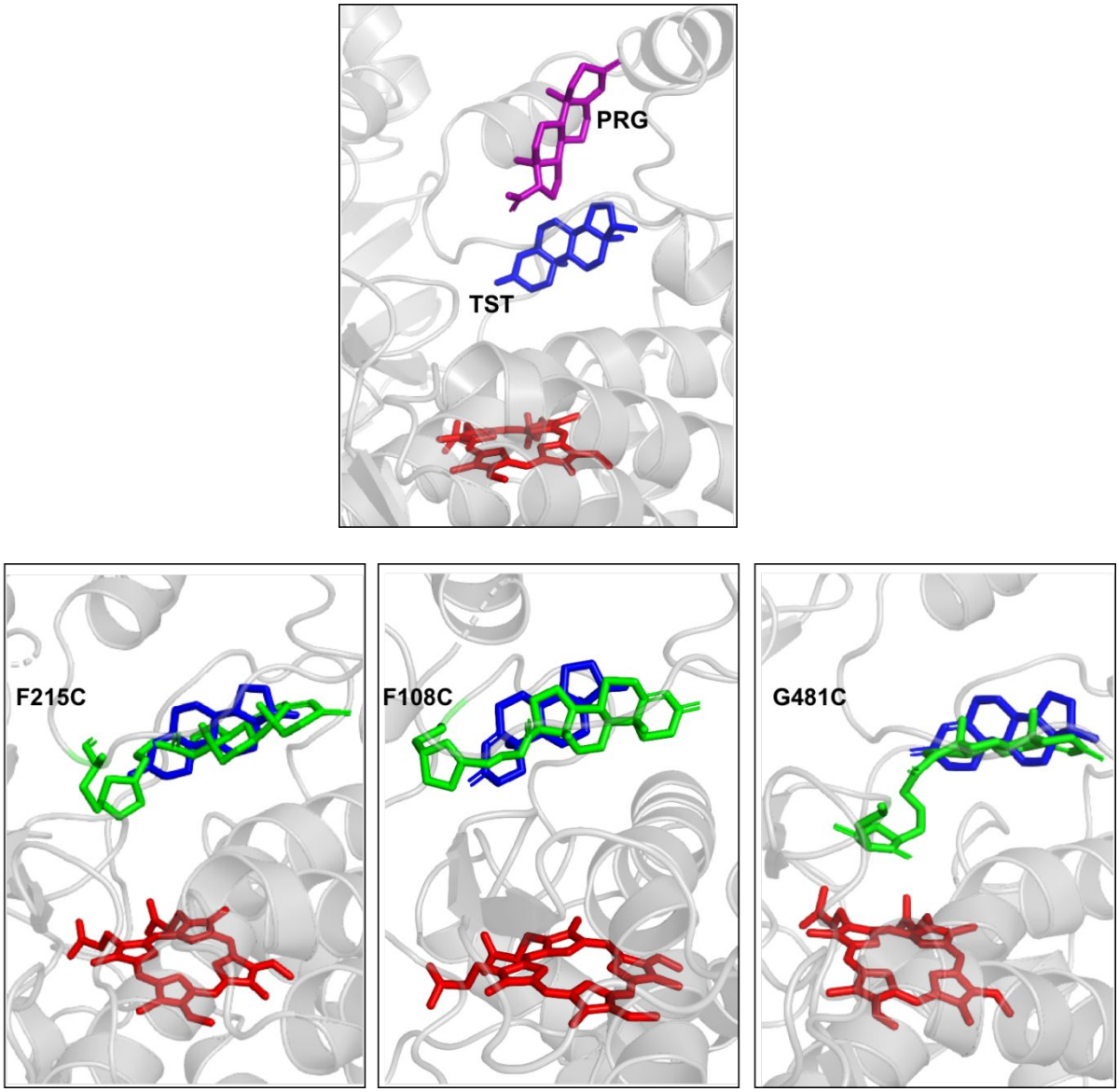


**Figure S9.** Binding orientation of the PGM moiety of different bioconjugates compared to a temporary binding site reported for testosterone. *Top*: in purple is the progesterone (PRG) co-crystallized with P450 3A4 (PDB: 1W0F)[5] and in blue is the testosterone (TST) bound in a temporary binding site identified by Hackett[7] in computational studies. *Bottom*: mut6 (F215C), mut1 (F108C), and mut2 (G481C) bioconjugated to PGM. The PGM moiety is oriented as best as possible to fit the temporary testosterone binding site. In all three cases, a good alignment was not achieved. Note that the orientation of the steroid ring system of PGM is flipped lengthwise compared to that of testosterone.

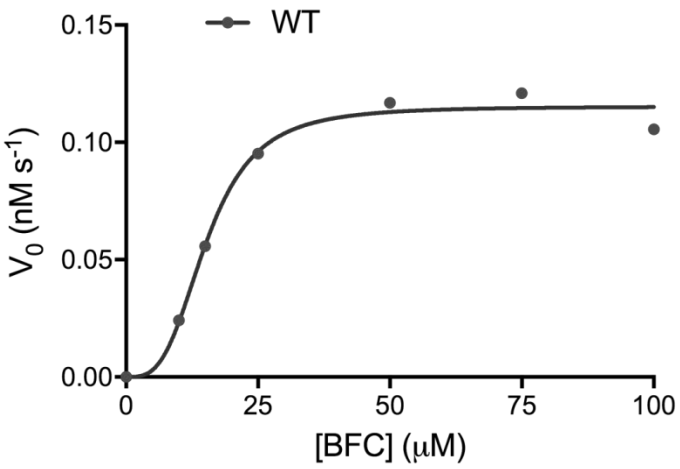


**Figure S10.** Michaelis-Menten BFC debenzylation kinetic curve for P450 3A4 WT. The experiment was done in triplicates. Error bars are smaller than the point size and are therefore not visible. The data points were curve fitted using the Hill equation (**Figure S14**). Refer to **Figure S12** for Hill coefficients.

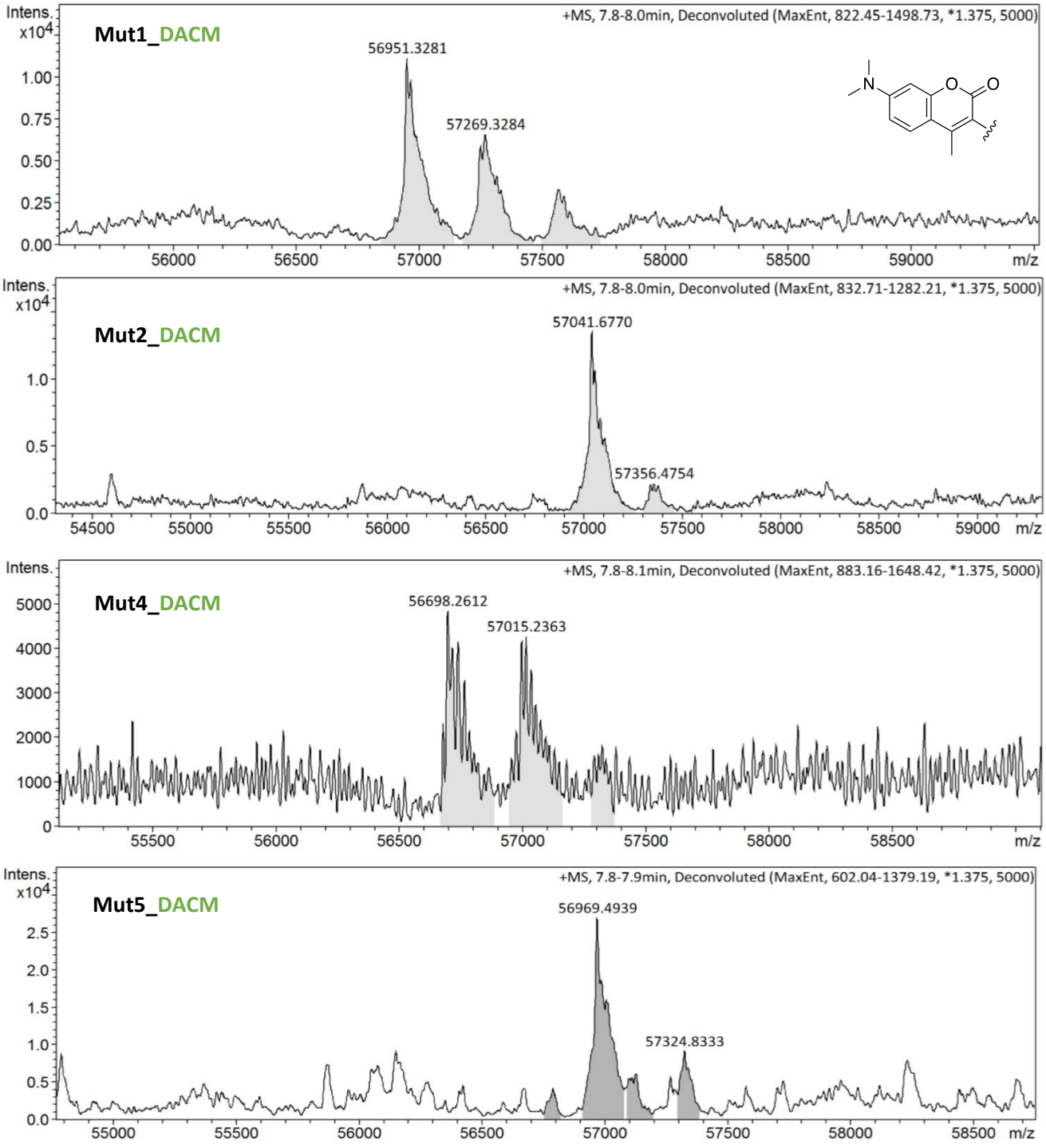


**Figure S11a.** Deconvoluted mass spectra of P450 3A4 mutants labeled with DACM. Refer to Figure S3 for theoretical masses of the unlabeled mutants and the mass of DACM label. Peaks correspond either to the unlabeled or the DACM, single or multiple-labeled protein.

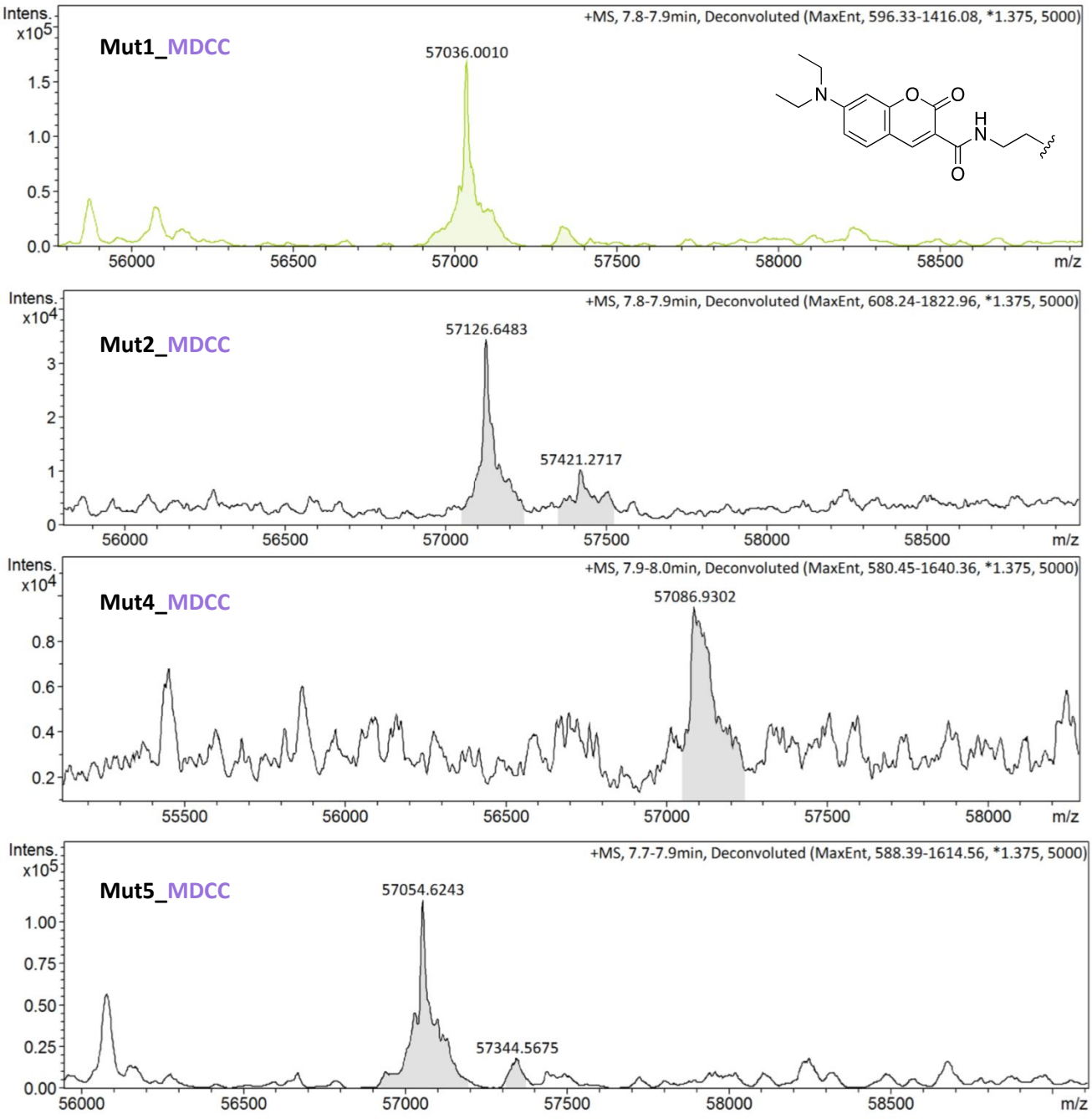


**Figure S11b.** Deconvoluted mass spectra of P450 3A4 mutants labeled with MDCC. Refer to Figure S3 for theoretical masses of the unlabeled mutants and the mass of MDCC label. Peaks correspond either to the unlabeled or the MDCC, single or multiple-labeled protein.

| Mutant | | DACM | | |
|---|---|---|---|---|
| | | 0 label | 1 label | 2 labels |
| Mut1 | % yield | 55 | 31 | 14 |
| | STD | 3 | 1 | 2 |
| Mut2 | % yield | 0 | 84 | 16 |
| | STD | 0 | 3 | 3 |
| Mut3 | % yield | 27 | 56 | 17 |
| | STD | - | - | - |
| Mut4 | % yield | 48 | 35 | 18 |
| | STD | - | - | - |
| Mut5 | % yield | 62 | 38 | 0 |
| | STD | 4 | 4 | 0 |

| Mutant | | MDCC | | |
|---|---|---|---|---|
| | | 0 label | 1 label | 2 labels |
| Mut1 | % yield | 0 | 100 | 0 |
| | STD | - | - | - |
| Mut2 | % yield | 0 | 77 | 23 |
| | STD | - | - | - |
| Mut4 | % yield | 0 | 100 | 0 |
| | STD | - | - | - |
| Mut5 | % yield | 0 | 86 | 14 |
| | STD | - | - | - |

**Figure S11c**. DACM and MDCC bioconjugation yields. The % yield was calculated from obtaining the peaks intensity ratio, assuming that the different labeling event do not significantly affect the ionization capabilities of the labeled protein. The standard deviation is determined from duplicates samples unless indicated by a dash.

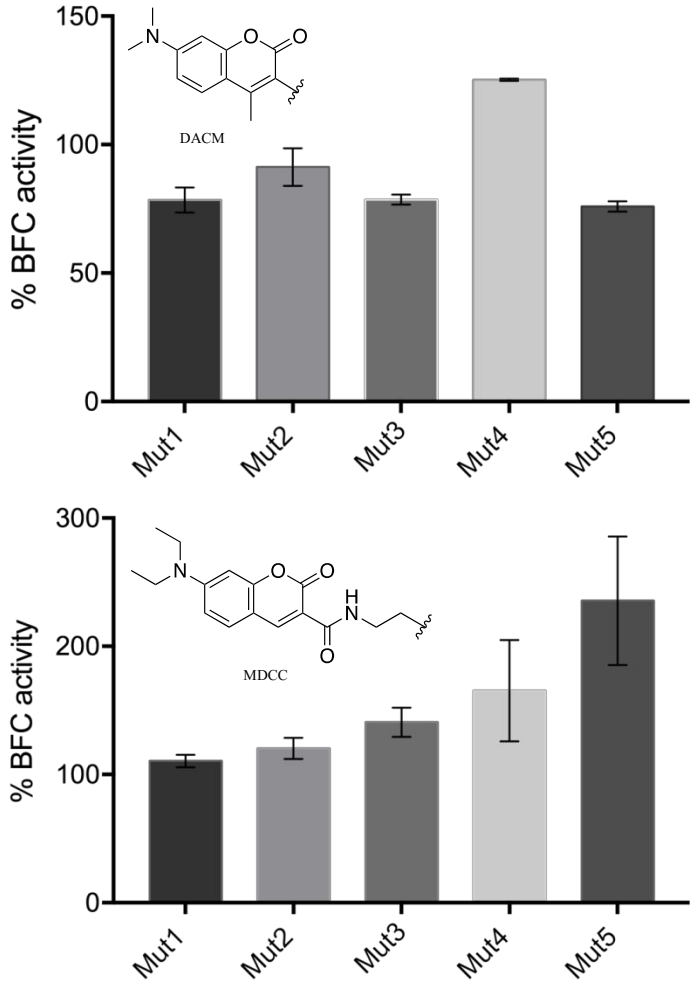


**Figure S11d.** Coumarin-maleimides bioconjugation effect on P450 3A4 mutants' activity towards BFC debenzylation. The activity ratio was calculated by comparing the linear portion of the HFC production curves of the labeled vs. unlabeled mutant. *Top:* Impact of DACM conjugation to BFC activity of P450 3A4 mutants. The assay contained 16.5 μM BFC, 0.4 μM P450, 3.2 μM CPR, and 1 mM NADPH. DACM did not improve BFC turnover except for a slight increase observed for mut4. The error bars represent standard error of triplicates. *Bottom:* Impact of MDCC conjugation to BFC activity of P450 3A4 mutants. The assay contained 33 μM BFC, 0.8 μM P450, 0.8 μM CPR, and 1mM NADPH. MDCC did not improved BFC turnover of mut1 and mut2. A slight increase in BFC activity was observed for mut3 and a more significant one for mut4 and mut5. The error bars represent standard error of triplicates.

| Mutants | n |
|---|---|
| Mut1 | 2.4 ± 0.4 |
| Mut1_PGM | 2.2 ± 0.5 |
| Mut2 | 1.7 ± 0.2 |
| Mut2_PGM | 1.8 ± 0.3 |
| Mut3 | 1.7 ± 0.3 |
| Mut3_PGM | 1.7 ± 0.4 |
| Mut4 | 2.0 ± 0.3 |
| Mut4_PGM | 1.6 ± 0.2 |
| Mut5 | 1.2 ± 0.2 |
| Mut5_PGM | 1.4 ± 0.1 |
| Mut6 | 1.4 ± 0.4 |
| Mut6_PGM | 2.0 ± 0.6 |
| WT | 3.2 ± 0.3 |

**Figure S12.** Hill coefficients (n) of PGM labeled and unlabeled mutants derived from the BFC kinetics (Figure 3). All mutants, PGM labeled and unlabeled, show BFC cooperativity. Error represents standard error of triplicates.

| Mutation | Primer sequence |
|---|---|
| F108C (Mut1) | 5′-CCACTGGACCACAAGGCCTCCGGTTTGT-3′ |
| G481C (Mut2) | 5′-CCCCTGAAATTAAGCTTAGGATGCCTTCTTCAACCTGAAAAACCC-3′ |
| L482C (Mut3) | 5′-CCCTGAAATTAAGCTTAGGAGGATGTCTTCAACCTGAAAAACCCG-3′ |
| V111C (Mut4) | 5′-CACAAACCGGAGGCCTTTTGGTCCATGCGGATTTATGAAAAGTGCC-3′ |
| Q484C (Mut5) | 5′-CTAGAAATTAAGCTTAGGACTTCTTTGCCCTGAAAAACCCGTTGTTCTAAAGG-3′ |
| F215C (Mut6) | 5′-GAAAACACCAAGAAGCTTTTAAGATTTGATTGTTTGGATCCATT CTTTC-3′ |
| I301C (Mut7) | 5′-TCATAGCCAGCAAAAATAAAGCAAATTGATTGGGCCACGAGCTC-3′ |
| F304C (Mut8) | 5′-GTTTCATAGCCAGCACAAATAAAGATAATTGATTGGGCCACGAGC-3′ |
| L210C (Mut9) | 5′-CCCCTTTGTGGAAAACACCAAGAAGTGTTTAAGATTTGATTTTTTGGATCCA-3′ |
| I120C (Mut10) | 5′-TCCAGTGGGATTTATGAAAAGTGCCATCTCTTGCGCTGAGGATGAAGAAT-3′ |
| G109C (Mut11) | 5′- CACAAACCGGAGGCCTTTTTGTCCAGTGGGATTTA-3′ |

**Figure S13** Primer list of all designed P450 3A4 mutants. Only the forward primers are shown.

**Hill equation**:

$$V_0 = V_{max} S^n / (K_M^n + S^n)$$

$V_0$= rate of HFC production (nM $s^{-1}$)
$V_{max}$= maximum rate of HFC production (nM $s^{-1}$)
S= BFC concentration ($\mu$M)
$K_M$= BFC affinity constant ($\mu$M)
n= Hill coefficient

**One phase decay equation**:

$$Y = (Y_0 - \text{Plateau}) \exp(-K * X) + \text{Plateau}$$

Y= rate of HFC production (nM $s^{-1}$)
X= concentration of PRG ($\mu$M)
$Y_0$= initial rate of HFC production (nM $s^{-1}$)
K= rate constant ($\mu M^{-1}$)
Plateau= Y corresponding to the plateau

**Plateau followed by one phase decay equation**:

$$Y = \text{if } (X<X_0, Y_0, \text{Plateau} + (Y_0 - \text{Plateau}) \exp(-K * (X - X_0)))$$

Y= rate of HFC production (nM $s^{-1}$)
X= concentration of PRG ($\mu$M)
$Y_0$= average HFC production rate of the plateau (nM $s^{-1}$)
$X_0$= PRG concentration at which the decay begins ($\mu$M)
K= rate constant ($\mu M^{-1}$)
Plateau= Y corresponding to the plateau

**Figure S14.** Equations from Prism 7 used to fit kinetic and PRG activation data.

## References


(1) Polic, V.; Auclair, K. Allosteric Activation of Cytochrome P450 3A4 via Progesterone Bioconjugation. *Bioconjug. Chem.* **2017**, *28* (4), 885–889.

(2) Domanski, T. L.; Liu, J.; Harlow, G. R.; Halpert, J. R. Analysis of Four Residues within Substrate Recognition Site 4 of Human Cytochrome P450 3A4 : Role in Steroid Hydroxylase Activity and a -Naphthoflavone Stimulation. *Arch. Biochem. Biophys.* **1998**, *350* (2), 223–232.

(3) Gillam, W. A. J. and E. M. J. Measurement of P450 Difference Spectra Using Intact Cells. In *Cytochrome P450 Protocols, Methods in Molecular Biology*; Al., I. R. P. et, Ed.; Springer Science+Business Media: New York, 2013; Vol. 987, pp 295–314.

(4) Ménard, A.; Huang, Y.; Karam, P.; Cosa, G.; Auclair, K. Site-Specific Fluorescent Labeling and Oriented Immobilization of a Triple Mutant of CYP3A4 via C64. *Bioconjug. Chem.* **2012**, *23* (4), 826–836.

(5) Williams, P. A.; Cosme, J.; Vinkovic, D. M.; Alison, W.; Angove, H. C.; Day, P. J.; Clemens, V.; J.T, I.; Jhoti, H. Crystal Structures of Human Cytochrome P450 3A4 Bound to Metyrapone and Progesterone. *Science (80-. ).* **2004**, *305* (5684), 683–686.

(6) Polic, V.; Sevrioukova, I. F.; Auclair, K. Steroid Bioconjugation to a CYP3A4 Allosteric Site and Its e Ff Ect on Substrate Binding and Coupling Efficiency. **2018**, *653* (May), 90–96.

(7) Hackett, J. C. Membrane-Embedded Substrate Recognition by Cytochrome P450 3A4. *J. Biol. Chem.* **2018**, *293* (11), 4037–4046.